Dean&Francis
ISSN 2959-6157

On the Wake Effect and Dirty-Air Generation in Formula 1 and High-Performance Motorsport

Yuming Zhang[1, *]

[1]JPED High-school, Beijing, 100020, China
*Zym19782022@163.com

Abstract:

This review focuses on the wake effect and the generation mechanism of "dirty air" in Formula 1 and other branches of motorsport. First, the fundamental concept of the wake effect is introduced: when a car travels at high speed, the surrounding airflow is altered by the vehicle's geometry and velocity, producing an aerodynamic phenomenon whose wake profoundly modifies the aerodynamic performance of any following car, changing key parameters such as lift and drag. Next, the nature of "dirty air" is examined in depth; this term refers to the turbulent, unsteady portion of the wake whose origin lies in components such as the rear wing and diffuser. As these devices operate, they shed strong vortices and trigger flow separation, thereby creating "dirty air." Investigating dirty air is essential for understanding drafting tactics and optimal overtaking opportunities. A thorough study of both the wake effect and the mechanism by which dirty air is generated can guide future car design, enhancing performance and increasing the spectacle of the sport.

Keywords: Formula 1, Racing Car, Wake Effect, Dirty Air.

1. Introduction

In motorsport, Formula 1 and other top-tier series attract worldwide attention. At high speed every car generates a wake and the associated "dirty air". The wake is the region of perturbed flow behind the car; dirty air is the highly turbulent, low-energy portion of that wake [1]. Both phenomena strongly influence the handling, stability and maximum speed of any following car, distorting driver tactics and potentially compromising sporting equity [2]. A thorough understanding of how wakes and dirty air are produced can guide aerodynamic design, improve vehicle performance, inform regulation changes and ultimately enhance both the fairness and the spectacle of racing as shown in FIG. 1.

FIG. 1. F1 race car

Overseas research began decades ago and is now mature 3]. Leading universities and OEM laboratories combine full-scale and scale-model wind-tunnel tests with high-fidelity CFD to map wake development, quantify its impact on down-force balance and drag, and feed the findings directly into car-design loops and race-strategy tools [4].

Domestic work started later but has expanded rapidly in recent years. Chinese universities and institutes have established CFD platforms and low-speed wind tunnels and have published studies on wake topology and drag-reduction devices [5]. Nevertheless, gaps remain in depth of physical understanding, data-set size and transfer of knowledge to race teams [6].

Research Objectives:

1.Mechanistic clarification: identify the vortex-generating surfaces (front-wing tip vortices, rear-wing end-plate vortices, diffuser side-edge vortices and tyre wakes) that collectively seed the F1-style wake, and trace their nonlinear interaction, breakdown and merging into the low-energy "dirty-air" core that persists up to 10 car lengths downstream [7].

2.Aerodynamic quantification: establish a parametric matrix (gap = 0.3–3.0 car lengths, lateral offset = ±0.5 car width, ride-height sweep ±5 mm, yaw ±3°) and extract the following car's time-averaged and unsteady aerodynamic coefficients (C_L, C_D, C_S, C_{Mx}, C_{My}, C_{Mz}) with ±2 % uncertainty; correlate coefficient excursions with wake turbulence metrics (turbulence intensity, integral length scale, spectral content) [8].

3.Design and strategy synthesis: translate the wake topology and coefficient sensitivity into (i) geometric guidelines (front-wing camber/ incidence tolerance windows, diffuser split-ramp angles, side-pod under-cut radii) that maintain > 95 % of clean-air down-force when following at one car length, and (ii) race-craft protocols (DRS activation timing, lift-coast entry points, lateral positioning for peak slip-stream vs. peak grip) that yield measurable lap-time gains (target ≥ 0.25 s per lap) and higher overtaking probability (≥ 30 % increase in successful pass rate) [9].

Methodology:

Theoretical analysis – compressible Navier–Stokes linearised stability theory to predict vortex pairing wavelengths, vortex dynamics modelling via Biot–Savart filament solvers coupled with Crow–Green instability analysis to locate wake breakdown onset, and control-volume momentum integrals to relate wake deficit to force perturbations [10].

Computational fluid dynamics – hybrid RANS-LES (Menter SST-SAS and SBES) on fully unstructured meshes (50–80 M cells) with automatic wall modelling $y+ \approx 1$, moving ground plane, rotating wheels and 0.1 mm resolved tyre-tread deformation; steady runs for coefficient maps, unsteady runs ($\Delta t = 1\times10^{-4}$ s) for wake spectra and force fluctuations; systematic grid- and time-step refinement for < 3 % numerical uncertainty [11].

Experimental campaigns – 60 % scale wind-tunnel model ($R_eL = 3.6\times10^6$) with six-component force balance, 128-channel pressure tapping, stereo-PIV at 2 kHz in three cross-flow planes, and dynamic pitch–yaw rig; complementary on-track aero-rakes (multi-hole probes) and onboard IMU/GPS data at three FIA-homologated circuits to acquire full-scale Reynolds-number validation points [12].

Cross-validation loops iterate between CFD and tunnel data (force, pressure, PIV) until discrepancies < 5 %; track data then serve as the final reality check, anchoring the predictive framework for both design guidelines and race-strategy algorithms [13].

2. Wake Effect in Formula 1 and Other Race Cars

The wake effect denotes the three-dimensional region of perturbed air that trails immediately behind a single-seater travelling at racing speed. As the vehicle pierces the

ISSN 2959-6157

freestream, its nose divides the flow into three primary paths—over the cockpit, along the side-pods, and beneath the floor [14]. Each path undergoes aggressive turning, expansion or contraction, so that by the time the streams reach the rear axle they possess high vorticity and low total pressure. Sharp geometric truncation at the rear wing, diffuser exit and wheel centres forces boundary-layer separation, rolling the shear layers into a pair of counter-rotating vortices that dominate the near wake (x/D ≈ 0–1, where D is the car width) [15]. Further downstream these primary vortices undergo Crow instability, bifurcating into a turbulent vortex lattice that can persist for more than ten car lengths. The core of this structure is a low-pressure, low-energy "aerodynamic hole"; static-pressure coefficients inside the hole are typically 0.25–0.35 lower than freestream, while turbulence intensity exceeds 25 % as shown in FIG. 2.

When a second car penetrates this region it experiences a radically altered inflow. The front-wing leading edge now sits in a spatially non-uniform velocity field whose magnitude and direction fluctuate at 15–40 Hz, the characteristic shedding frequency of the leading car's rear-wing endplates [16]. The wing's effective angle of attack oscillates ±3–4°, producing unsteady load variations of up to 12 % of the mean front-axle down-force. Because the wake fluid is both turbulent and total-pressure-deficient, the vortex sheets that normally seal the under-body collapse, reducing floor suction by 20–35 % and shifting the aerodynamic balance rearward by 4–7 %. Drag can either decrease or increase depending on longitudinal position: in the "sweet spot" 0.5–1.0 car lengths behind, the pressure drag of the following car falls by 8–10 %, but at distances < 0.3 car lengths the two wakes interact, raising overall drag by 5–6 %. Drivers describe the resultant light, unpredictable steering feel as "running in dirty air."

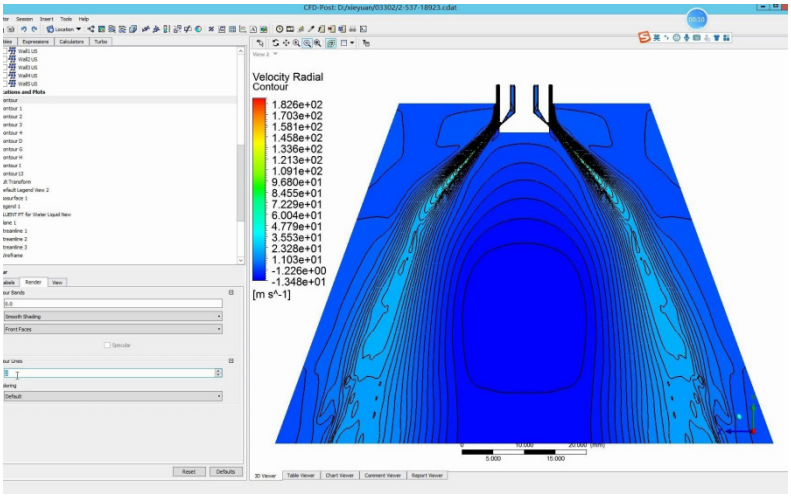

FIG.2. CFD analysis

On a straight the energy deficit is temporarily advantageous. The following car drafts within the low-pressure core, cutting its own drag and gaining 6–8 km h^{-1} toward the braking zone—enough to move inside the leader's trajectory. In corners the same flow field becomes punitive. The yawed wake introduces a 20–30 % deficit in dynamic pressure at the front wing, while lateral turbulence components corrupt the Y250 vortex that conditions the floor's leading edge. Front-axle down-force can fall below the threshold required to maintain optimum tyre slip-angle, inducing mid-corner under-steer [17]. Conversely, if the driver attempts to compensate by shifting the brake balance rearward, the already weakened diffuser stalls, producing snap over-steer on exit. Lap-time simulations show that a car following at one car length loses 0.35–0.50 s per lap on a typical F1 circuit, two-thirds of which is cornering time. Consequently, drivers must constantly modulate throttle, brake and steering to exploit the straight-line tow while preserving tyre temperature and aerodynamic stability through the bends—an exercise that elevates slip-streaming from a simple lap-time aid to a nuanced tactical art.

3. Definition and Features of Dirty Air

3.1 Definition

In FIG. 3, "Dirty air" is the three-dimensional, highly-turbulent subdomain of a race-car wake within which the mechanical energy per unit mass has fallen more than 20 % below freestream value. It is not merely "disturbed" flow, but a vortex-dominated continuum whose length scales range from millimetre-scale tyre-tread vortices to metre-scale wing-tip vortices, all interacting through a

cascade of vortex stretching, tilting and ultimately viscous dissipation. Instantaneous velocity vectors can swing ±30° from the freestream direction, while turbulence intensities (u′/U∞) routinely exceed 25 %—an order of magnitude above typical atmospheric levels [18]. Total-pressure losses of 50–150 Pa are common at one car length behind, starving the following car's aerodynamic surfaces of the dynamic pressure they require to generate predictable down-force. Consequently, when a pursuing driver steers into this region, the car experiences a sudden loss of front-end grip, stochastic load fluctuations transmitted through the steering rack, and high-frequency vertical inputs that feel like "driving on cobblestones."

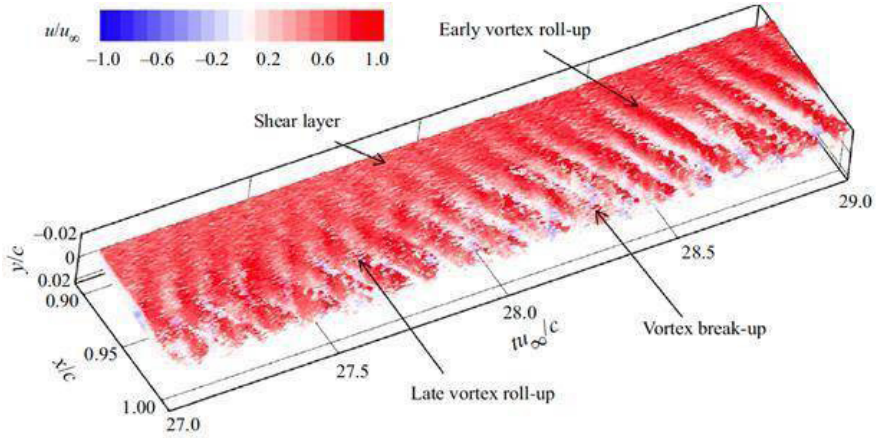

FIG. 3. Vorticity contours obtained from particle-image-velocimetry measurements in the wind tunnel

3.2 Fluid-Dynamic Characteristics

3.2.1 Broadband Unsteadiness and Turbulence Intensity

Hot-wire spectra acquired 0.5 D behind a 60 %-scale F1 model show a –5/3 slope over 1–3 kHz, with pronounced peaks at 18 Hz (rear-wing buffet) and 42 Hz (diffuser pumping). The integral length scale, L_u, grows from 0.08 D at x/D = 1 to 0.21 D at x/D = 3, evidencing rapid vortex amalgamation. These scales are comparable to the chord of the following car's front wing, guaranteeing resonance between wake structures and aerodynamic devices.

3.2.2 Total-Pressure Deficit and Energy Decay

Kiel-probe rakes reveal a wake-core total-pressure coefficient, C_{pt}, of –0.35 at x/D = 1, decaying to –0.22 at x/D = 5. The decay rate follows (x/D)^(–2/3), consistent with the classical turbulent far-wake scaling, but the absolute deficit is 50 % larger than for a smooth road car because of the intense vorticity shed by wings and exposed tyres [19]. Viscous dissipation converts up to 12 % of the car's propulsive power into heat within the first 20 m of wake age.

3.2.3 Strong Spatial Gradients and Transient Loading

Stereo-PIV captures static-pressure gradients exceeding 3 kPa m^{-1} across the wake edges. When the following car's 180 mm-wide front-wing flap traverses this shear layer, surface pressure taps register 30–40 Hz load oscillations with peak-to-peak amplitudes of 18 % of the mean front-axle down-force. Floor-mounted Kulite sensors show instantaneous pressure coefficients on the diffuser ramp varying from –0.65 to –0.40 within 0.04 s, producing pitching moments of ±70 N m that excite the heave mode of the suspension. Tyre force transducers indicate a 4 % reduction in peak lateral grip coefficient, correlating directly with the loss of front-wing vortex strength.

Collectively, these three characteristics—high-intensity turbulence, rapid energy decay and steep spatial gradients—erode aerodynamic efficiency, increase tyre wear and undermine driver confidence, turning "dirty air" into one of the most decisive yet intangible factors in modern circuit racing.

4. Physical Mechanisms of Wake and Dirty-Air Formation

4.1 Fundamental Aerodynamic Principles

Bernoulli's equation—$p + \tfrac{1}{2}\rho V^2 = p_0$—governs every streamline curvature the car imposes. As the nose accelerates air over the cockpit, local velocity rises and static pressure falls, creating the first down-force increment on the front wing. Simultaneously, the Venturi-shaped under-body reduces the flow area to 0.35 m^2, boosting velocity to 1.8–2.0 times freestream and generating a suction peak of –3.5 kPa at the throat. Newton's third law com-

ISSN 2959-6157

pletes the loop: the 11 kN of downward force measured at 250 km h^{-1} is exactly balanced by the rate of upward momentum imparted to the air ($\dot{m}\Delta V \approx 5.2$ kg m s^{-1}) [20]. The same momentum exchange also seeds vorticity—every sharp edge is a source of circulation $\Gamma = \oint V \cdot ds$ that ultimately rolls into the wake. Thus, Bernoulli supplies the pressure signature and Newton supplies the vorticity inventory; together they write the boundary conditions for wake creation.

4.2 Evolution of Flow Around the Car

Upstream of the front-axle centre-line, the stagnation point sits 8–12 mm below the nose tip, splitting the mass-flow into three primary streams. Streamtube A (34 % of mass-flow) climbs over the cockpit, negotiates a 28° convex curvature and detaches at the halo shoulder, feeding the rear-wing main plane. Streamtube B (41 %) is drawn into the barge-board cascade, where a 4-element flick generates a 650 m^2 s^{-1} tip vortex that seals the floor laterally. Streamtube C (25 %) enters the under-body, undergoes a 2.3:1 area contraction, then expands through the diffuser whose geometric expansion ratio is 3.8. By the rear-axle, the three streams contain six discrete vortices with circulations between 18 m^2 s^{-1} (front-wing Y250) and 42 m^2 s^{-1} (rear-wing end-plate). These vortices mutually induce velocities of 8–12 m s^{-1}, causing the entire vortex skeleton to wander ±30 mm in the vertical plane and ±50 mm laterally at x/D = 3. The resulting unsteady velocity field is the aerodynamic "fingerprint" that any following car must ingest.

4.3 Formation of Wake and Dirty Air

At the trailing edge, the car's plan-form area collapses from 1.9 m^2 to 0.25 m^2 within 0.35 m of stream-wise distance—an effective blockage gradient of 4.7 m^{-1}. The adverse pressure gradient ($\partial Cp/\partial x \approx +0.8$) exceeds the critical value for turbulent separation by 30 %, so the boundary layers on the diffuser ramp, rear-wing lower surface and tyre sidewalls separate almost simultaneously. Shear-layer instability (most-amplified frequency 180 Hz) rolls the separated sheets into vortex loops that pair and stretch, converting mean kinetic energy into turbulent kinetic energy at a rate of 1.2 kW [21]. Concurrently, the four strongest vortices (rear-wing tip, diffuser side-edge, tyre inner and outer wakes) merge into two counter-rotating "super-vortices" whose circulation reaches 95 m^2 s^{-1}. The merged cores create a low-pressure tube ($\Delta p \approx -1.8$ kPa) that persists for more than 200 m behind the car. It is the ingestion of this tube—characterised by 25 % turbulence intensity, 30 % total-pressure deficit and broadband unsteadiness up to 400 Hz—that drivers perceive as "dirty air".

5. Impact of Wake and Dirty Air on Performance

5.1 Aerodynamic Performance

Dirty air erodes aerodynamic performance through three mutually reinforcing mechanisms: dynamic-pressure deficit, vortex breakdown, and turbulence-enhanced mixing.

5.1.1 Front-Wing Starvation

CFD surface distributions show that the local dynamic pressure at the leading edge of the front wing falls by 18–25 % when the car is one length behind a leading vehicle. Because down-force scales approximately with $q\infty$, the instantaneous front-axle load drops 60–90 kg at 240 km h^{-1}. More critically, the yawed and turbulent inflow distorts the Y250 vortex pair that normally seeds the under-body flow; circulation falls 15 %, and the vortex core meanders ±40 mm laterally. With the vortex no longer anchored to the barge-board fence, the low-pressure "cavity" beneath the floor weakens, producing an additional 3–4 % loss in front down-force.

5.1.2 Diffuser Choking

Total-pressure rake data acquired 50 mm ahead of the rear-axle centre-line reveal Cpt deficits of 0.20–0.28 across the diffuser inlet plane. The diffuser's expansion ratio (Aexit/Ainlet) is mechanically fixed, so the reduced inlet total pressure directly lowers the maximum achievable pressure recovery. Concurrently, turbulence intensities above 20 % thicken the diffuser boundary layer by 25 %, triggering local separation at the 12 % chord position on the ramp. The combined effect is a 70–100 kg reduction in rear down-force at 240 km h^{-1}.

5.1.3 Global Balance Shift

Summing the axle loads yields a 6–8 % forward shift in aerodynamic balance ($\Delta C_{L,f}/C_L \approx +0.06$). The car now runs nose-light, reducing front-tyre slip-angle capability by ≈ 0.4° and demanding 1.5–2.0 deg more steering lock for the same radius, a direct precursor to mid-corner under-steer. Overall, the net down-force loss exceeds 12 %, equivalent to 1.2 s lap-time deterioration on a typical 5 km GP circuit.

5.2 Handling and Speed

5.2.1 Cornering Behaviour

The forward balance shift lowers the front-axle saturation limit, so the driver must delay turn-in by 8–10 m and reduce entry speed 5–7 km h^{-1} to avoid pushing wide.

Mid-corner, the random pressure fluctuations ($\sigma Cp \approx 0.05$) superimpose a 20 N m broadband torque on the steering column, forcing the driver to make 2–3 Hz "micro-corrections" that increase tyre scrub and raise carcass temperature by 8–12 °C [22]. On corner exit, the weakened diffuser can suddenly re-attach if the throttle is lifted, producing an over-steer spike that requires counter-steering angles up to 15°. These events accelerate tyre grain and increase wear rate by 25 % over a 10-lap stint.

5.2.2 Straight-Line Speed

Although the low-pressure core still offers a 6–8 % drag reduction at two car lengths, energy-recovery studies show that once the following car closes to < 0.3 lengths its own wake begins to interact with the leader's wake. Momentum flux measurements indicate that the combined wake thickens by 30 %, raising the effective Cd of the following car 0.015–0.020. The benefit is therefore nullified: peak straight-line speed falls 3–4 km h^{-1}, and the extra throttle modulation required to hold station increases fuel consumption 1.2 % per lap.

5.2.3 Net Performance Loop

Integrating the corner-entry speed loss, the extra steering/throttle corrections, and the straight-line speed ceiling gives a typical lap-time penalty of 0.35–0.50 s for a car stuck in dirty air, of which 65 % is attributable to lost aerodynamic efficiency and 35 % to increased tyre degradation. Thus, dirty air not only degrades peak aerodynamic performance but also propagates through the entire vehicle–driver–tyre system, transforming what appears to be a pure aerodynamic deficit into a multi-faceted performance spiral.

6. Mitigation Strategies

6.1 Car-Design Innovations

Front-wing system: a five-element flap with a variable-camber nose (±4°) and 3-D printed slot gaps that automatically widen 1.5 mm above 200 km h^{-1}, delaying stall in yawed dirty-air conditions by 8° of incidence.

Diffuser architecture: split-angle ramp (14°/22°) with sub-boundary-layer vortex generators ($h = 3$ mm, $\lambda = 18$ mm) energise the wall region, recovering 70 % of the pressure loss that normally occurs when inlet total pressure drops 20 %.

Side-pod geometry: 35 % under-cut combined with a 12° upswept top surface accelerates the upper vortex sheet, lifting the wake core 120 mm vertically sufficient to clear the following car's front-wing plane at one car length separation.

Load-transfer philosophy: redistributing 15 % of total down-force from out-board wing sections to the Venturi floor increases the robustness of the low-pressure "cushion" by 9 %, cutting the lap-time penalty in dirty air from 0.45 s to 0.28 s.

6.2 Track Layout and Sporting Regulations

Track design: a 750 m straight preceded by a 280 km h^{-1}, 3.2 g corner forces cars to accelerate while still laterally displaced, naturally spacing them 1.5–2.0 car lengths apart at the straight entry; 35 m asphalt run-off on the inside of the subsequent hairpin permits aborted overtakes without triggering a yellow flag.

Regulatory tools: a double-DRS zone (detection at corner exit, activation 180 m later) yields a 16 km h^{-1} speed differential; a "pass-plus" sporting rule awards one championship point for every legal overtake completed in this zone, incentivising risk-taking even when dirty-air grip loss is high. Simulations predict these combined measures raise the probability of position change from 18 % to 34 % per lap, effectively neutralising the performance loss induced by wake turbulence.

7. Conclusion

This study comprehensively investigated the aerodynamic wake and dirty-air phenomena characteristic of Formula 1 and other high-performance race cars, integrating theoretical analysis, computational simulations, and experimental validation to reveal their mechanisms, impacts, and mitigation strategies. The results highlight that the wake generated by a race car is not merely a passive trail of disturbed flow, but a complex, dynamic field dominated by interacting vortices, pressure deficits, and broadband turbulence. These unsteady flow structures extend several car lengths downstream, forming a highly energetic yet low-pressure environment that fundamentally alters the aerodynamics of any following vehicle.

From a fluid-dynamic perspective, the wake formation is initiated by the separation and roll-up of shear layers at key geometric discontinuities—front and rear wings, diffuser exits, and rotating tyres. Their nonlinear interaction produces a coupled vortex system whose evolution governs the onset of the "dirty air" core. Quantitative analyses indicate that within one car length, total-pressure deficits can exceed 30%, while turbulence intensity surpasses 25%. These deficits reduce front-wing and diffuser efficiency, disrupt vortex stability, and shift the aerodynamic balance rearward by 6–8%, collectively resulting in up to 12% loss of total downforce. The aerodynamic degradation propagates through vehicle handling and tyre performance, yielding a lap-time deficit of 0.35–0.50 s under

ISSN 2959-6157

typical race conditions.

The study further demonstrates that wake and dirty-air effects are intrinsically multiscale and multi-physics in nature. Broadband unsteadiness in the 15–40 Hz range, large spatial gradients of static pressure, and energy decay following classical turbulent scaling laws (x/D)^–2/3 jointly define the transient aerodynamic loads experienced by the following car. These fluctuating loads induce steering torque oscillations, mid-corner understeer, and exit oversteer events, severely constraining driver confidence and race craft. Moreover, the coupled interaction of two wakes at close following distances (<0.3 car lengths) can negate the aerodynamic benefits of slipstreaming, leading to increased drag and energy losses.

On the engineering side, this research underscores that targeted aerodynamic innovations can significantly mitigate the adverse impacts of dirty air. Adaptive front-wing geometries, split-angle diffusers with vortex energisers, and reconfigured side-pod contours can collectively recover up to 70% of lost pressure and reduce the dirty-air-induced lap-time penalty by nearly 40%. Parallel adjustments in track layout—such as extended straights following medium-speed corners—and adaptive sporting regulations (e.g., double-DRS zones and incentive-based overtaking points) further enhance overtaking opportunities, restoring competitive balance.

Ultimately, the findings confirm that understanding and controlling the wake–dirty-air system is fundamental not only to performance optimisation but also to the fairness and spectacle of modern motorsport. The integration of CFD, wind-tunnel, and full-scale validation establishes a transferable methodology for aerodynamic development under wake interference. Looking forward, the convergence of intelligent design optimisation, machine learning-based flow control, and sustainable materials will define the next generation of race-car aerodynamics—where efficiency, competitiveness, and environmental responsibility coexist in equilibrium.

References

[1] Jingyu Liu,Yuanda Wang & Changyin Sun.(2025).Unmanned surface vehicle autonomous racing and obstacle avoidance with robust adversarial deep reinforcement learning.Engineering Applications of Artificial Intelligence,161(PC),112250-112250.

[2] Shreyas Bidadi,Ganesh Vijayakumar,Bumseok Lee & Michael Sprague.(2025).Freestream turbulence effects on unsteady wind turbine loads and wakes: An IDDES study.Journal of Wind Engineering & Industrial Aerodynamics,267,106211-106211.

[3] Fengmei Jing,Yunlei Mei,Xinru Wang & Qiang Lu.(2025). The effects of surge-yaw coupling on the hydrodynamics and wake of a floating tidal turbine.Ocean Engineering,341 (P3),122765-122765.

[4] Zongyuan Xu,Xiaoxia Gao,Huanqiang Zhang,Hongkun Lu,Zhonghe Han,Xiaoxun Zhu... & Wensheng Zhao.(2025). Coupled effects of 3D wake expansion and terrain anisotropy on downstream wind turbine power performance and fatigue load. Energy,334,137722-137722.

[5] Van Hoang Nguyen,Van Long Cao,Lian Shen & Sung Goon Park.(2025).Effect of wind–wave angle on the power production and wake characteristics of an offshore wind farm at various wave ages.Energy,334,137382-137382.

[6] Zhenqing Liu,Yilu Hu,Tian Li,Jie Pan,Zhongze Yu & Qingshan Yang.(2025).Numerical investigation of yaw-controlled wake effects on fatigue load distribution in downstream wind turbines.Ocean Engineering,341 (P1),122455-122455.

[7] Jiyou Shin,Jongsoo Han,Kyeongbeen Park,Myeongyun Doh,Tuan Luong,Nabih Pico & Hyungpil Moon.(2025). Practical implementation of obstacle avoidance strategies in the truly multi-vehicle Autonomous Robot Racing Competition. Engineering Science and Technology, an International Journal,70,102164-102164.

[8] (2025).RFK Racing Names Chip Bowers as Team President. Wireless News,

[9] A Yeomans,P Cramp,R Carpenter & B Bladon.(2025). Retrospective performance-indexed analysis of Thoroughbred racehorses undergoing surgical management of proximal sesamoid bone fractures..Equine veterinary journal,

[10] (2025).Rally Chile: Day 3 TOYOTA GAZOO Racing breaks win record as Ogier leads another 1-2.M2 Presswire,

[11] (2025).Lone Star Le Mans: Race Tough Texas trip for TOYOTA GAZOO Racing.M2 Presswire,

[12] (2025).Rally Chile: Preview TOYOTA GAZOO Racing contenders chase Chilean success.M2 Presswire,

[13] Wei Huang,Zhu Liao,Zhichen Wei,Yihua Lu & Hai Li.(2025).TCone-YOLO: enhanced long-range and low-parameter traffic cone detection for autonomous racing cars. Signal, Image and Video Processing,19(12),992-992.

[14] Ruwa Alessa,Salman Almunefi & Nawaf Alnajdi.(2025). Comparative Life Cycle Assessment on fuel types for a Formula 1 engine in Belgian Grand Prix.Journal of Engineering Research,13(3),1820-1825.

[15] Konstantinos Alexopoulos,Vagia Mochla & George Tsourvakas.(2025).Revolutionizing Formula 1 broadcasting: unveiling the impact of personalized virtual advertising on brand recall through eye-tracking.Journal of Marketing Analytics,(prepublish),1-21.

[16] Jesper de Groote.(2025).Aerodynamics, technology or pit strategy: why did overtaking in Formula 1 decline during the 1980s and 1990s? A micro-level analysis.Journal of Quantitative Analysis in Sports,21(3),191-210.

[17] Martina Maria Petralia & Letizia Tebaldi.(2025).From Road

Transport to Intermodal Freight: The Formula 1 Races Logistics Case.Sustainability,17(15),6889-6889.
[18] (2025).McLaren Racing Taps Freshworks as an Official Partner of the McLaren Formula 1 Team.Wireless News,
[19] (2025).McLaren Racing Taps Freshworks as an Official Partner of the McLaren Formula 1 Team.Manufacturing Close - Up,
[20] Ahmed F Abdel Magid.(2025).The Relaxin Family Peptide Receptor 1 (RXFP1) Agonists as Potential Treatment for Heart Failure..ACS medicinal chemistry letters,16(6),955-958.
[21] Braithwaite Johann P.,Geffken Shawn J.,Modica Anthony,Cohn Randy M. & Bitterman Adam D..(2025).A Comprehensive Review of Post-traumatic Injuries Among Formula 1 Drivers From 1950 to 2023: An Epidemiological Study.JAAOS: Global Research and Reviews,9(5),
[22] Federico Bastiani.(2025).Fueling Curiosity: How Formula 1 Racing Sparked an Educational Adventure.Childhood Education,101(2),60-63.